Available online at www.sciencedirect.com
SCIENCE DIRECT®
International Journal of Mass Spectrometry 237 (2004) 1–12
International Journal of Mass Spectrometry
www.elsevier.com/locate/ijms

Formation of $C_6H_nSi^+$ (n = 5–8) from phenylsilane: an experimental and theoretical study

Joong Chul Choe*

Department of Chemistry, University of Suwon, P.O. Box 77, Suwon 440-600, Korea

Received 20 May 2004; accepted 23 June 2004

Abstract

The metastable ion decomposition (MID) spectra of $C_6H_nSi^+$ (n = 6–8) generated by electron ionization of phenylsilane were obtained using mass-analyzed ion kinetic energy spectrometry (MIKES). H and H_2 losses were the main channels in the MID of $C_6H_8Si^{\bullet+}$ (**1**). The dominant product ion in the MIDs of $C_6H_7Si^+$ (**2**) and $C_6H_6Si^{\bullet+}$ (**3**) was $C_6H_5Si^+$ (**4**) formed by H_2 and H losses, respectively. Density functional theory calculations were performed to investigate isomerizations and dissociations of **1**–**3** at the B3LYP/6-311++G(d,p) level. RRKM model calculations were performed to understand their dissociation kinetics. These theoretical results predict that the consecutive dissociation **1** → **3** (+ H_2) → **4** + $H^{\bullet}$ dominates at low energies, while **1** → **2** (+ $H^{\bullet}$) → **4** + H_2 at high energies. It has been found that several isomers of **1**–**3** including ion–molecule complexes, $C_6H_6{\cdot}SiH_x^+$ (x = 0–2), play important roles in the dissociation of **1**. Reaction mechanisms are proposed for the formation of several isomers of **1**–**4** from the phenylsilane molecular ion.

Keywords: Phenylsilane ion; Metastable ion decomposition; DFT calculation; RRKM calculation

1. Introduction

Organosilicon ions have been the subject of very interesting mass spectrometric studies [1–18]. Their behavior can be similar to or very different from that of their corresponding carbon analogues. Dissociations of aromatic organosilicon ions are less well understood than those of aliphatic ions studied recently by several researchers [14–18]. Compared to the extensive work on the toluene molecular ion, studies on the dissociation of the phenylsilane were scarce until the appearance of recent reports by Beauchamp and co-workers [5,6] using Fourier transform-ion cyclotron resonance (FT-ICR) spectrometry. After their reports in which the formation of silacycloheptatrienyl ion, the silicon analogue of the tropylium ion, from the phenylsilane ion was suggested, the dissociation of phenylsilane ion has been studied using several methods including high resolution electron ionization (EI) mass spectrometry [10], FT-ICR [9], collision-induced dissociation (CID) [10], and quantum chemical calculations [7–9].

In an early EI study by Schwarz and co-workers [4], hydrogen scrambling in the dissociation of deuterium-labeled phenylsilane ion was observed, similar to the dissociation of toluene ion. In the EI mass spectrum of toluene [19], the $[M-1]^+$ peak is prominent with a considerable abundance of the molecular ion, $M^{\bullet+}$. By contrast, the abundances of $[M-2]^{\bullet+}$ and $[M-3]^+$ are considerable as well as $[M-1]^+$ and $M^{\bullet+}$ in the EI mass spectrum of phenylsilane [10,19]. This provides an opportunity to investigate the difference between the two molecular ions. It is well known that the benzyl and tropylium ions are the main products in the dissociation of toluene ion [20]. By contrast, the formation of several structural isomers was suggested for $C_6H_8Si^{\bullet+}$ (**1**), $C_6H_7Si^+$ (**2**) and $C_6H_6Si^{\bullet+}$ (**3**) by EI of phenylsilane [5,6,9]. The suggested isomers include phenyl-containing ions $C_6H_5SiH_x^+$, ion–molecule complexes $C_6H_6{\cdot}SiH_x^+$, and ions containing a seven- or five-membered ring. Important isomeric structures

* Tel.: +82 31 220 2150; fax: +82 31 222 9385.
E-mail address: jcchoe@suwon.ac.kr (J.C. Choe).

1387-3806/$ – see front matter © 2004 Elsevier B.V. All rights reserved.
doi:10.1016/j.ijms.2004.06.008

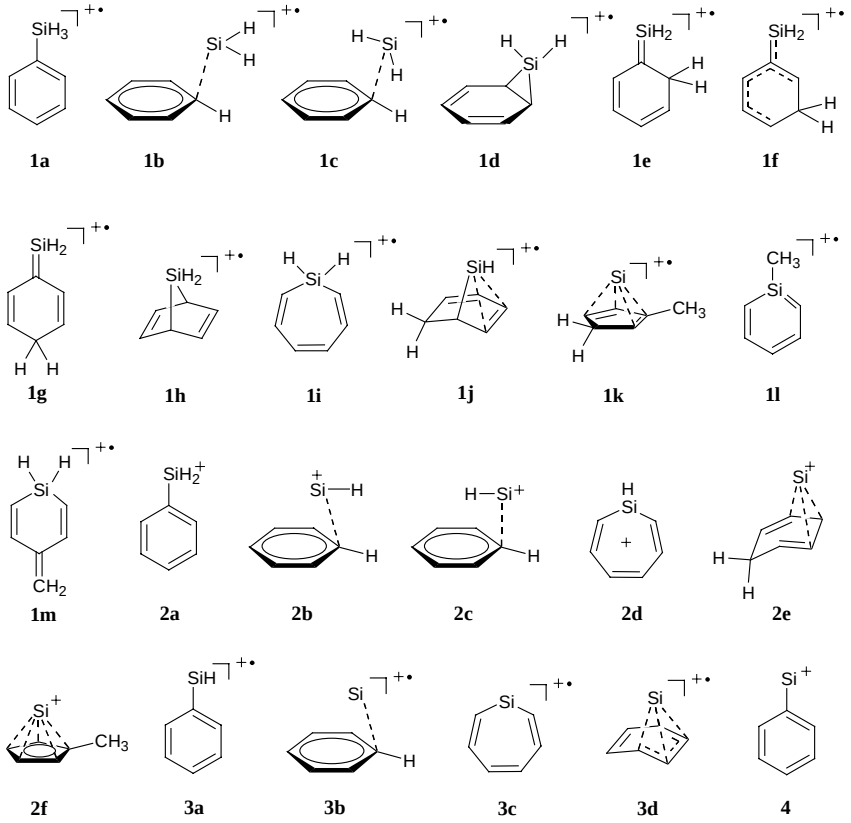

Fig. 1. Schematic representation of structures **1**–**4**. For abbreviations, see Tables 1 and 2.

are shown schematically in Fig. 1. Allene and Lampe [11] and Bohme et al. [12] reported formation of stable complexes by reactions between benzene and SiH_x^+. Schwarz and co-workers [13] obtained three stable structures (**3a**, **3b**, **3c**) for **3** using ab initio molecular orbital calculations and suggested the presence of **3a** and **3b** from the neutralization-reionization spectra. Beauchamp and co-workers [5,6] investigated the reactions of $C_6H_nSi^+$ (n = 5–8) generated by EI of phenylsilane with phenylsilane or benzene-d_6 using FT-ICR. They proposed two structures (**1a**, $C_6H_6{\cdot}SiH_2^+$) for **1**, two (**2a**, **2d**) for **2**, three (**3a**, **3b**, **3c**) for **3**, and one (phenylsilylidyne ion) for $C_6H_5Si^+$ (**4**). These ions include the ion–molecule complexes ($C_6H_6{\cdot}SiH_2^+$, **3b**) and the seven-membered structures (**2d**, **3c**). Nicolaides and Radom [8] calculated theoretically eight isomers of **2** and concluded that **2a** and **2f**, the latter of which contains a five-membered ring, are the most probable candidates for **2** generated by EI of phenylsilane. A further study to determine the structure for **2** was carried out by Jarek and Shin [9] using FT-ICR and quantum chemical calculations. Their result agrees with that of Beauchamp and co-workers for the first structure (phenylsilyl ion, **2a**), the silicon analogue of the benzyl ion and called the 'reactive' isomer because of its reactivity with other molecules. They proposed, however, an ion–molecule complex (**2b**) as the second structure, called the 'unreactive' isomer because of its lack of reactivity with other molecules. To summarize, the three groups [6,8,9] suggested three different isomers (**2b**, **2d**, **2f**) for the unreactive $C_6H_7Si^+$ ion, while they agreed for the reactive isomer (**2a**).

In a recent study in this laboratory [10] using high resolution and CID mass spectrometry, an attempt was made to elucidate the overall dissociations of the phenylsilane ion. Besides the products formed by consecutive H and/or H_2 losses and ring cleavages, the productions of $C_6H_7^+$ and $C_6H_6^{\bullet+}$ via ion–molecule complexes and $C_5H_4Si^+$ via the ion (**1k**) containing a five-membered ring were proposed. For the unreactive $C_6H_7Si^+$ ion, both the structures **2b** and **2f** were suggested. The interpretation of the experimental data was based on usual chemical intuition.

In the present work, density functional theory (DFT) calculations have been carried out to investigate the formation of $C_6H_nSi^+$ (n = 5–8) in the ionization of phenylsilane. This includes several isomerizations and dissociations by H or H_2 losses of each ion. Unimolecular ion dissociation, or metastable ion decomposition (MID) can provide useful information in understanding of ionic dissociation kinetics because MID generally occurs somewhat above the reaction threshold. MID data can be used efficiently in evaluation of the energetics obtained from quantum chemical calculations, especially when exact experimental data such as rate measurements for dissociation of energy-selected ions are not available as in this case [21–23]. The MIDs of $C_6H_nSi^+$ (n = 6–8) generated by EI of phenylsilane have been obtained using mass-analyzed ion kinetic energy spectrometry (MIKES)

[24]. On the basis of the experimental and theoretical results, reaction mechanisms for the formation of isomeric $C_6H_nSi^+$ (n = 5–8) ions will be discussed.

2. Methods

2.1. Experimental

MID experiments were performed using a double focusing mass spectrometer with reverse geometry (VG Analytical ZAB-E) at Seoul National University. Phenylsilane was introduced into the ion source via a septum inlet and ionized by 70 eV EI. The ion source temperature was maintained at 140 °C, and ions generated were accelerated to 8 keV. MIKES was used to observe the MID of the ions generated in the ion source. A precursor ion was selected by the magnetic sector and the translational kinetic energy of a product ion generated in the second field-free region of the instrument was analyzed by the electric sector. To improve the quality of a MIKE spectrum, signal averaging was carried out for repetitive scans. Phenylsilane was purchased from Aldrich and used without further purification.

2.2. Computational

Molecular orbital calculations were performed with the Gaussian 98 suite of programs [25] using an IBM SP Nighthawk-2 computer at the Computer Center of Seoul National University. Geometry optimizations for the several isomeric $C_6H_nSi^+$ (n = 5–8) ions and related fragments were carried out at the B3LYP density functional levels of theory using the 6-311++G(d,p) basis set. Transition state (TS) geometries connecting important stable structures were searched. All the TS geometries found, other than **TS2a2b**, were checked by calculating the intrinsic reaction coordinates (IRCs) at the same level. The IRC calculation for **TS2a2b** was successful at the 6-31+G(d) level. For the odd-electron ions, the unrestricted B3LYP (UB3LYP) method was used. Spin contamination was satisfactory. All the expectation values for the spin operator $\hat{S}^2$ were in the range of 0.75–0.77. The harmonic vibrational frequencies and the zero-point energies for the optimized structures were calculated at the B3LYP/6-311++G(d,p) level. These have not been scaled because the appropriate scaling factor at this level is not known though that of 0.9614 was recommended for the B3LYP/6-31G(d) level [26].

The following RRKM expression [27] was used to calculate the rate constant k for various reactions involved

$$k(E) = \sigma \frac{W^{\neq}(E - E_0)}{h\rho(E)} \quad (1)$$

where E and E_0 are the reactant internal energy and the critical energy for the reaction, respectively, $W^{\neq}$ the sum of states at TS, ρ the density of states of the reactant, and σ the reaction path degeneracy.

3. Results and discussion

3.1. Experimental observations

In the 70 eV EI mass spectrum of phenylsilane obtained here, the relative abundances of the peaks at m/z 108, 107, 106, 105, 104, and 103 are 100, 97, 89, 55, 1, and 4, respectively. The low abundances of the latter two mean that the m/z 105 ion is relatively stable or dissociates by channels other than H and H_2 losses, such as ring cleavages, which have not been considered in this work. In the MID of the phenylsilane molecular ion at m/z 108, the main products were the m/z 107 and 106 ions, due to H and H_2 losses, respectively. To investigate further dissociations of these fragment ions, MID experiments were carried out for the m/z 107 and 106 ions generated in the ion source. The main products in the MID of m/z 107 ion were the m/z 106 and 105 ions. The m/z 105 ion was dominant in the MID of the m/z 106 ion. These MID-MIKE spectra are shown in Fig. 2.

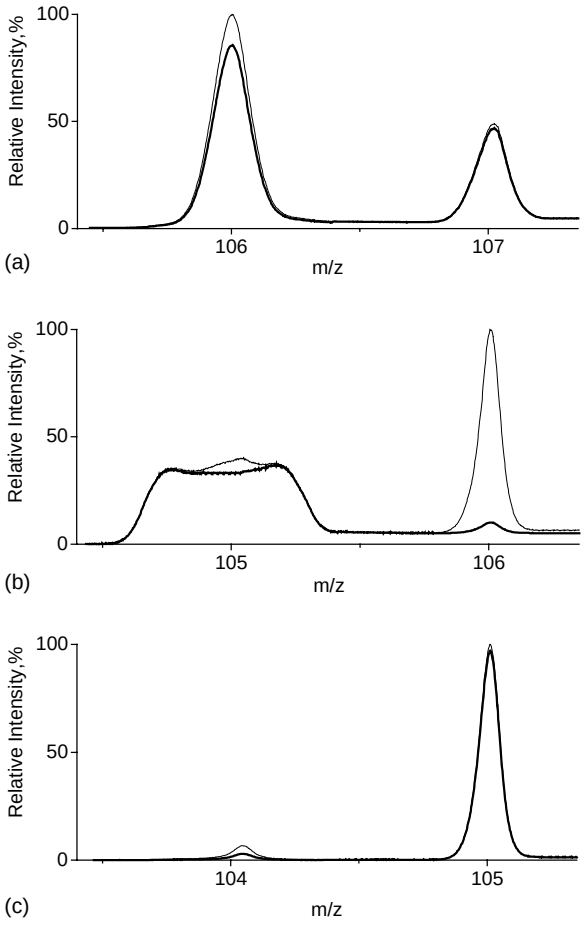

Fig. 2. MID-MIKE spectra of the ions at: (a) m/z 108; (b) m/z 107; and (c) m/z 106 generated by EI of phenylsilane. Thin lines denote the raw data. Thick lines denote the results corrected for isotopic contributions of A-1 and A-2 peaks, which correspond to the MIDs of: (a) $C_6H_8Si^{\bullet+}$; (b) $C_6H_7Si^+$; and (c) $C_6H_6Si^{\bullet+}$. See text for details.

Care is needed in interpreting such spectra, however, when considerable amounts of A-1 and/or A-2 type ions are generated in the ion source because their isotopic ions can contribute significantly to the signal for an A ion [28]. For example, the peak at *m*/*z* 106 mainly consists of $^{12}C_6H_6{}^{28}Si^{\bullet+}$, $^{13}C_6H_5{}^{28}Si^{+}$, $^{12}C_6H_5{}^{29}Si^{+}$, and $^{12}C_6H_4{}^{30}Si^{\bullet+}$ with relative abundances of 100: 6.6: 5.1: 3.4, respectively. The ions with the most abundant isotopes corresponding to these ions appear at *m*/*z* 106, 105, 105, and 104, respectively. The contributions from the latter three ions to the MID of the *m*/*z* 106 ion were subtracted. (Fig. 2c) The MID spectra of the genuine ions of **2** and **1** free from the isotopic contributions were obtained consecutively in the same way. (Fig. 2) It appeared that isotopic contributions significantly affected the MID of **2** (Fig. 2b). Before subtracting the isotopic contributions, the *m*/*z* 105 peak consists of narrow and broad components, and the abundances of the *m*/*z* 105 and 106 peaks are comparable. After subtracting, however, the narrow component of the *m*/*z* 105 peak disappears, and more importantly is that the *m*/*z* 106 peak is reduced to a negligible peak. This is due to the large difference between the MID yields of the *m*/*z* 107 and 106 ions. The latter was 3.2 times larger than the former. Almost all of the product *m*/*z* 106 ions in the MID of the *m*/*z* 107 ion originate from the isotopic contribution of **3**. These reconstructed MID data lead to the conclusion that metastable **1** dissociates mainly by H_2 and H losses with a branching ratio (measured by peak areas) of 2.8:1, and the main dissociation channels of **2** and **3** are the production of **4** by H_2 and H losses, respectively.

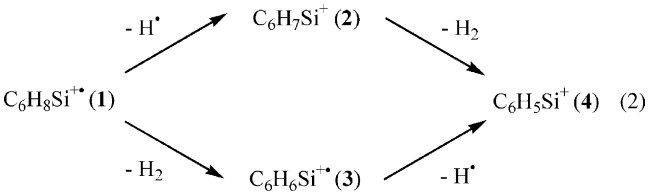

(2)

3.2. DFT calculations

Three research groups have carried out quantum chemical calculations on the phenylsilane ion and related species. Nicoliades and Radom [8] proposed various isomeric structures for neutral C_6H_8Si and calculated their energies at several levels. The energies calculated for some isomeric **2** ions were reported also. Jarek and Shin [9] calculated the energies for some isomeric **1** and **2** ions. Their calculations for **1** were performed at the restricted open-shell HF (ROHF) and MP2 (ROMP2) levels. Energies for **1a**, **1b**, **1d**, **1i**, and **1h** were obtained and a TS connecting **1a** and **1b** was optimized. Schwarz and co-workers [13] reported calculated results on **3a**, **3b**, and **3c**. In the present study, stable isomeric and TS structures for $C_6H_nSi^+$ (n = 5–8) were optimized with the B3LYP/6-311++G(d,p) DFT calculations. For odd-electron ions (**1**, **3**), calculations were performed at the unrestricted B3LYP (UB3LYP) level.

Table 1
Relative energies in kJ mol^{-1} of $C_6H_8Si^{\bullet+}$ ions calculated at the UB3LYP/6-311++G(d,p) DFT level

Species		Symmetry	ΔE^a
1a	Phenylsilane$^{\bullet+}$	C_S	0.0
1b	$C_6H_6{\cdot}SiH_2{}^{\bullet+}$	C_S	12.9
1c	$C_6H_6{\cdot}SiH_2{}^{\bullet+}$	C_1	−1.9
1d	Slianocaradiene$^{\bullet+}$	C_S	−6.1
1e	*o*-Isophenylsilane$^{\bullet+}$	C_S	5.0
1f	*m*-Isophenylsilane$^{\bullet+}$	C_1	57.0
1g	*p*-Isophenylsilane$^{\bullet+}$	C_{2V}	−0.3
1h	7-Silanorbornadiene$^{\bullet+}$	C_{2V}	66.2
1i	Silacycloheptatriene$^{\bullet+}$	C_{2V}	41.1
1j	$C_6H_7{\cdot}SiH^{\bullet+}$	C_1	71.3
1k	(η^4-Methylcyclopentadiene)silicon$^{\bullet+}$	C_1	14.5
1l	α-Silatoluene$^{\bullet+}$	C_S	−73.7
1m	4-Methylenesilacyclohexadiene$^{\bullet+}$	C_{2V}	39.8
TS1a1b		C_S	74.0
TS1a3a		C_1	128.2
TS1b1c		C_1	15.8
TS1b1e		C_1	98.1
TS1b1h		C_S	91.8
TS1b3a		C_1	158.6
TS1b3b		C_1	174.7
TS1c1d		C_1	−1.8
TS1d1i		C_1	101.6
TS1d1j		C_1	155.0
TS1e1f		C_1	93.8
TS1f1g		C_1	97.9
TS1i3c		C_S	197.2

[a] Energy at the zero point referred to that of **1a**. Zero-point energies were added to calculate the relative energies. The calculated total energy and zero-point energy of **1a** are −522.7007028 and 0.112066 hartrees, respectively.

3.2.1. Isomerization and dissociation of $C_6H_8Si^{\bullet+}$

The relative energies for several isomeric **1** ions and the TSs optimized are listed in Table 1, and some important geometrical structures are shown in Fig. 3. Two structures for the phenylsilane ion were found. The more stable one (**1a**) has a Si–H bond in the plane of the phenyl ring. The other (**1a′**) has a Si–H bond in a plane orthogonal to the phenyl ring. Frequency calculations show that **1a** corresponds to a local minimum, while **1a′**, a rotational TS that can be assigned as the six-fold barrier to internal rotation of the SiH_3 group. The energy difference between the two is very small (0.17 kJ mol^{-1}). Interestingly, the neutral molecule with **1a** structure has been calculated to be a TS, while that with **1a′** structure to be a local minimum according to a theoretical study by Portalone et al. [29].

1a can isomerize to **1b** by a 1,2 shift of an α-H atom from the silicon to the *ipso*-carbon. The relative energy (74 kJ mol^{-1}) of **TS1a1b** is smaller than the energy (128 kJ mol^{-1}) needed for the dissociation of **1a** to **3a** by 1,1-H_2 elimination, the lowest energy channel in the dissociation of **1**. (Fig. 4) In this paper, the abbreviation **TSxy** will be used to represent the transition state connecting **x** and **y**, optimized for the lowest energy path. **1b** can transform to several stable isomers. It can isomerize to a more stable ion **1d** via **1c**. The barriers between **1b** and **1d** are very low. **1b** can isomerize to another more stable ion **1e** by a 1,2-H shift

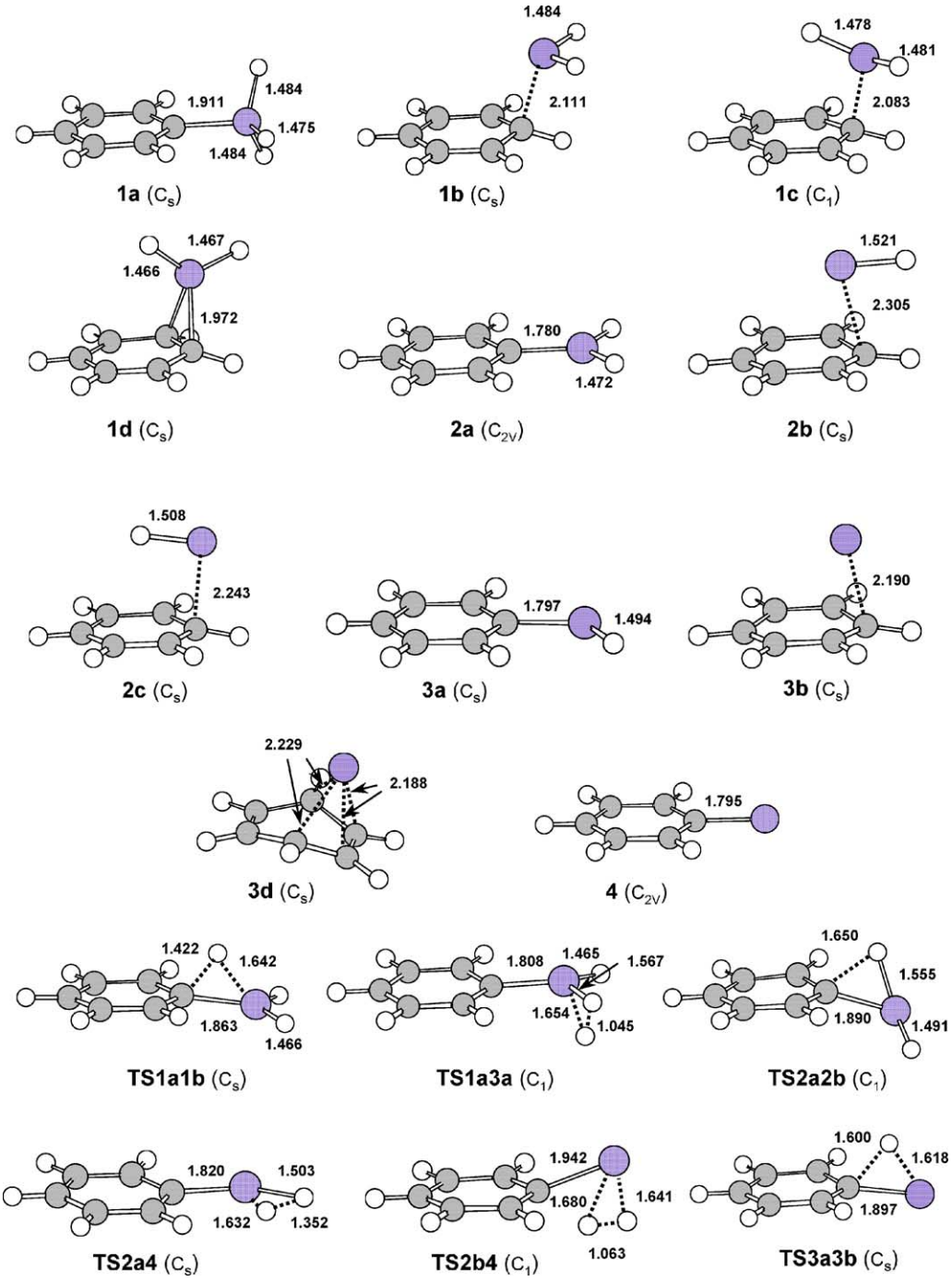

Fig. 3. Geometrical structures for selected species optimized at the B3LYP/6-311++G(d,p) DFT level. The numbers are the bond lengths in Å. The molecular symmetry is denoted in parentheses.

from the *ipso* to the *ortho*-carbon, but with a considerable barrier (85 kJ mol^{-1}). **1e** can subsequently undergo two 1,2-H shifts to form **1f** and **1g** (Fig. 1). **1b** can isomerize to a less stable ion **1h**. **1d** can undergo a further isomerization to form a seven-membered ring in ion **1i**. By a 1,4 shift of an α-H atom, **1d** can form another isomer **1j**. Its barrier, however, is very high (161 kJ mol^{-1} above **1d**) and lies above **TS1a3a** so that the isomerization **1d** → **1j** will not occur among the metastable ions.

We attempted to search and found a pathway from **1a** to **1k** because Nicolides and Radom [8] suggested the formation of isomers containing a five-membered ring (such as **1k**), and their suggestion was supported by our previous CID work [10]. To reach **1k**, the intermediate **1j** should undergo various isomerization steps. The highest barrier along the pathway lies 285 kJ mol^{-1} above **1a**, far higher than the energy (128 kJ mol^{-1}) for **TS1a3a**. This means that the formation of isomers containing a five-membered ring cannot compete

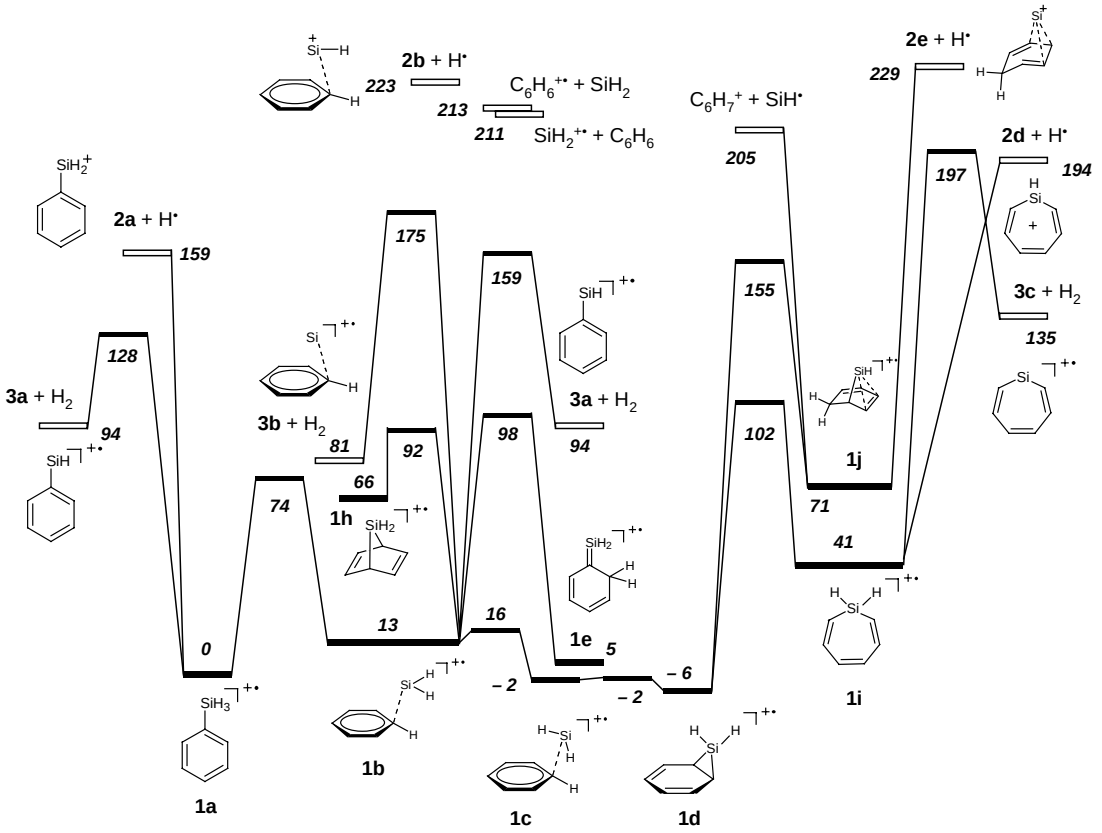

Fig. 4. Potential energy diagram for the isomerization and dissociation of $C_6H_8Si^{\bullet+}$ derived from the B3LYP/6-311++G(d,p) calculations. The italic numbers are the potential energies in kJ mol^{-1} at the zero point referred to that of **1a**.

with the direct dissociation of **1a**. Other possible stable isomers include **1l** and **1m**. Formation of these isomers from **1a**, however, is also expected to proceed via considerable energy barriers, although **1l** is the most stable among the investigated isomers of **1** (Table 1).

H_2 eliminations can occur from isomers other than **1a**. The barrier for 1,1-H_2 elimination from **1b** to produce **3b** is higher than for 1,2-H_2 elimination to produce **3a**, although **3b** is more stable than **3a**. Another possible H_2 elimination is the production of **3c** from **1i** by 1,1 elimination. All these H_2 elimination channels are energetically unfavorable compared to **1a** → **3a** + H_2.

For H losses from the isomers of **1**, TSs could not be located, suggesting loose transition states. The relative energies of the H loss products **2a**–**f** are listed in Table 2. The lowest energy channel from **1a** is the production of **2a** + H$^{\bullet}$. Although **2f** is found to be the most stable among the isomers of **2**, which can be produced from the five-membered isomer **1k** by H loss, occurrence of this H loss starting from **1a** is far less probable because of the presence of the very high barrier between **1a** and **1k**.

At low energies **1a** undergoes rapid interconversion to **1b**, **1c**, and **1d** as will be described in Section 3.3. Dissociations of **1b**, **1c**, and **1d**, however, by losses of H_2, H, C_6H_6, SiH_2, and SiH directly or via further isomerizations to **1i** or **1j** are energetically less favorable than the direct dissociations of **1a** to **2a** + H$^{\bullet}$ and **3a** + H_2. (Fig. 4) This indicates that **2a** and **3a** are predominantly produced in the primary dissociation of **1**. This seems to be in conflict with the previous suggestions [6,9] that several isomers of **2** and **3** are produced. It is possible, however, that **2a** and **3a** undergo isomerizations after their formation. It is to be noted that the rapid interconversion of **1a**, **1b**, **1c**, and **1d** at low energies can explain the H scrambling in **1** [9] and in its dissociation [4] observed in earlier deuterium labeling studies.

3.2.2. *Isomerization and dissociation of $C_6H_7Si^+$*

Fig. 5 shows the potential energy diagram for the isomerization and dissociation of **2a**. The relative energies for related species are listed in Table 2. **2a** can isomerize to **2b** by a 1,2 shift of an α-H atom from the silicon to the *ipso*-carbon. The isomerization barrier is lower than the barrier for the production of **4** by 1,1-H_2 elimination. **4** can be produced more easily from **2b** by 1,2-H_2 elimination. **2b** can isomerize to a rotational conformer **2c** prior to dissociation. **2b** undergoes easily 1,2-SiH migration to form a degenerate isomer. The barrier for the migration is very low, which lies 1.0 kJ mol^{-1} above **2b**.

2b can undergo other two isomerizations below or near its dissociation to **4** + H_2. One occurs by 1,3 shift of the α-H atom from the silicon to the *ortho*-carbon. The TS and the isomer lie 99 and 96 kJ mol^{-1} above **2b**, respectively. The other occurs

Table 2
Relative energies in kJ mol^{-1} of $C_6H_7Si^+$, $C_6H_6Si^{\bullet+}$, and $C_6H_5Si^+$ ions calculated at the B3LYP/6-311++G(d,p) DFT level

Species		Symmetry	ΔE[a]	ΔE (**1a**)[b]
$C_6H_7Si^+$				
2a	Phenylsilyl$^+$	C_{2V}	0.0	158.9
2b	$C_6H_6{\cdot}SiH^+$	C_S	64.4	223.3
2c	$C_6H_6{\cdot}SiH^+$	C_S	74.3	233.2
2d	Silacycloheptatrienyl$^+$	C_S	35.2	194.1
2e	(η^3-Cyclohexadienyl)silanium$^+$	C_S	70.2	229.1
2f	(η^5-Methylcyclopentadienyl)silanium$^+$	C_S	−49.6	109.3
TS2a2b		C_1	263.1	422.0
TS2a4		C_S	278.7	437.6
TS2b2c		C_1	99.5	258.4
TS2b4		C_1	220.8	379.7
$C_6H_6Si^{\bullet+}$				
3a	Phenylsilylene$^{\bullet+}$	C_S	0.0	93.5
3b	$C_6H_6{\cdot}Si^{\bullet+}$	C_S	−13.0	80.5
3c	Silacycloheptatrienylene$^{\bullet+}$	C_{2V}	41.9	135.3
3d	(η^4-Cyclohexatriene)silicon$^{\bullet+}$	C_S	−16.5	77.0
TS3a3b		C_S	106.0	199.4
TS3b3d		C_1	−11.9	81.6
TS3b4		C_S	223.1	316.6
$C_6H_5Si^+$				
4	Phenylsilylidyne$^+$	C_{2V}	129.4[c] (194.8)	288.3

[a] Energy at the zero point referred to that of **2a** or **3a** for $C_6H_7Si^+$ or $C_6H_6Si^{\bullet+}$, respectively. Zero-point energies were added to calculate the relative energies.

[b] Energy of $C_6H_7Si^+ + H^\bullet$, $C_6H_6Si^{\bullet+} + H_2$, or $C_6H_5Si^+ + H^\bullet + H_2$ relative to **1a** for $C_6H_7Si^+$, $C_6H_6Si^{\bullet+}$, or $C_6H_5Si^+$, respectively.

[c] Energy of **4** + H_2 relative to **2a**. Value in parentheses is energy of **4** + $H^\bullet$ relative to **3a**. The calculated total energies of H and H_2 are −0.5022569 and −1.1795715 hartrees, respectively. The zero-point energy of H_2 is 0.010063 hartrees.

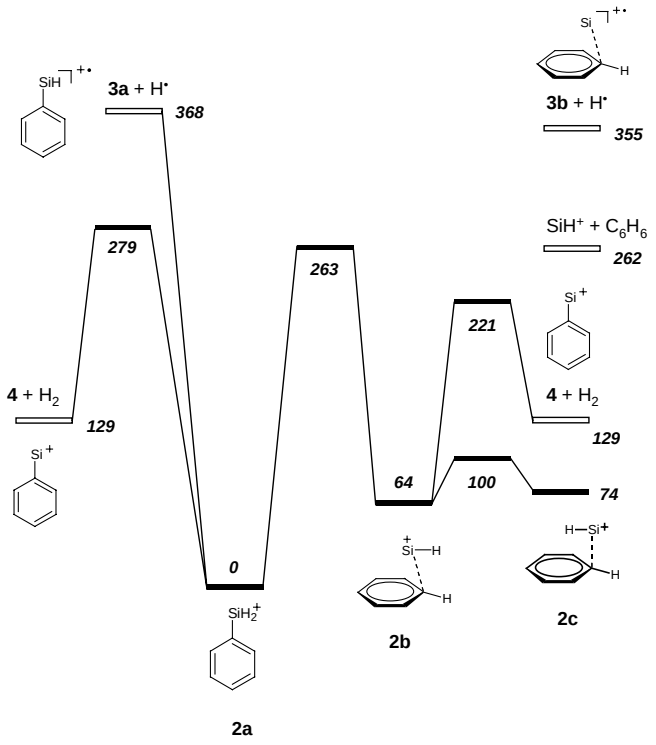

Fig. 5. Potential energy diagram for the isomerization and dissociation of $C_6H_7Si^+$ derived from the B3LYP/6-311++G(d,p) calculations. The italic numbers are the potential energies in kJ mol^{-1} at the zero point referred to that of **2a**.

by the Si insertion into a C–C bond to form a non-planar seven-membered $C_6H_7Si^+$ ion, which lies 88 kJ mol^{-1} above **2b**. The barrier for this Si insertion lies 3.8 kJ mol^{-1} above **TS2b4**. These isomerizations are energetically unfavorable compared to the isomerization to **2c**. The dissociation of **2b** by loss of benzene or H is energetically less favorable than the H_2 loss.

3.2.3. Isomerization and dissociation of $C_6H_6Si^{\bullet+}$

As in the cases of **1a** and **2a**, **3a** can undergo easily a 1,2 shift of the α-H atom from the silicon to the *ipso*-carbon to form an ion–molecule complex **3b**. (Fig. 6) The isomerization barrier is far lower than the threshold of **3a** → **4** + $H^\bullet$. **4** can be produced also from **3b** by loss of H via a TS located at 28 kJ mol^{-1} above the dissociation products. **3b** can isomerize readily to a more stable ion **3d** by slight movement of the Si atom toward the center of the ring. Similar with **2b**, **3d** can form a non-planar seven-membered isomer, but this is energetically unfavorable because of the presence of a considerable barrier lying 4 kJ mol^{-1} below **4** + $H^\bullet$. Pathways for H_2 loss from **3** that can compete with the H losses were not found, agreeing with the negligible detection of $C_6H_4Si^+$ in the MID of **3**.

3.3. RRKM model calculations

3.3.1. Primary dissociation

As mentioned above, the lowest energy channels for H and H_2 losses from **1** are **1a** → **2a** + $H^\bullet$ and **1a** → **3a** +

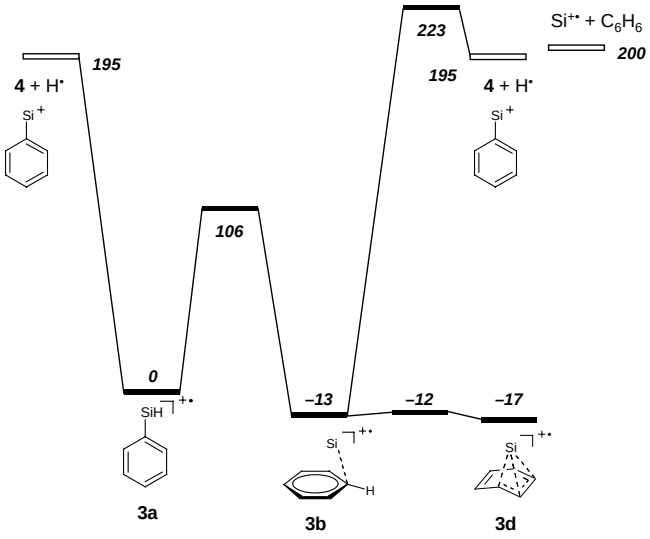

Fig. 6. Potential energy diagram for the isomerization and dissociation of $C_6H_6Si^{\bullet+}$ derived from the B3LYP/6-311++G(d,p) calculations. The italic numbers are the potential energies in kJ mol^{-1} at the zero point referred to that of **3a**.

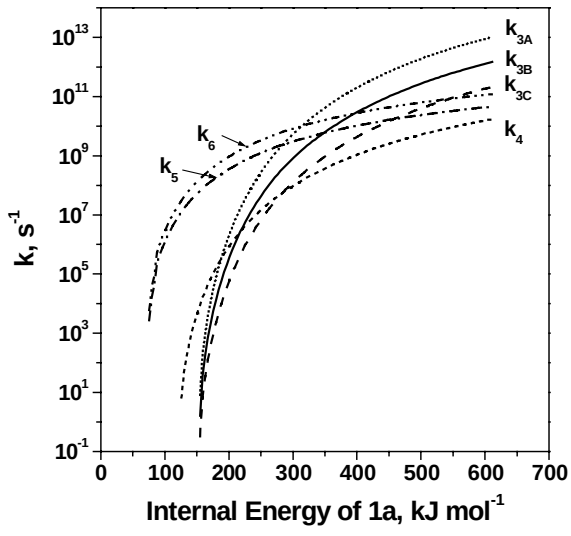

Fig. 7. RRKM rate constants for reactions 3–6 as a function of internal energy of **1a**. k_3–k_6 denote the rate constants for reactions 3–6, respectively. k_{3A}, k_{3B}, and k_{3C} denote the results calculated using $\Delta S^{\ddagger}_{1000\,K}$ of 46, 29, and 13 J mol^{-1} K^{-1}, respectively. See text for details.

H_2, respectively. Since the barrier for the isomerization **1a** → **1b** is lower than the dissociation barriers, the following four elementary reactions are important in the dissociation kinetics of **1**.

$$\mathbf{1a} \rightarrow \mathbf{2a} + H^{\bullet}, \quad k_3 \tag{3}$$

$$\mathbf{1a} \rightarrow \mathbf{3a} + H_2, \quad k_4 \tag{4}$$

$$\mathbf{1a} \rightarrow \mathbf{1b}, \quad k_5 \tag{5}$$

$$\mathbf{1b} \rightarrow \mathbf{1a}, \quad k_6 \tag{6}$$

The individual reaction rate constants were calculated using the RRKM formalism in Eq. (1). The critical energies of the reactions and the vibrational frequencies of precursors and TSs obtained with the DFT calculations were used in the RRKM rate calculations. The values of reaction path degeneracy (σ) used in the calculations of k_3–k_6 are 3, 6, 3, and 1, respectively. The internal rotation of the SiH_3 group of **1a** was taken into account in the calculations of k_3 and k_4. The frequency corresponding to a torsional vibration 32 cm^{-1} of **1a** was omitted, and the rotational constant for the internal rotation, 2.8 cm^{-1} calculated from the optimized geometry was used.

One uncertainty in the calculation of k_3 is the TS for reaction 3, found to have no saddle point. It is well known that RRKM rate constants do not depend on individual vibrational frequencies but on activation entropy ($\Delta S^{\ddagger}$), which defines the degree of looseness of TS [27,30]. According to the data compiled by Lifshitz [30] and subsequent work, most of the $\Delta S^{\ddagger}$ values at 1000 K for reactions occurring via loose TS are in the range of 13–46 J mol^{-1} K^{-1} (3.0–11 eu). Therefore, to calculate k_3 the TS frequencies were adjusted for $\Delta S^{\ddagger}_{1000\,K}$ to become 46, 29 (the middle value of the range), or 13 J mol^{-1} K^{-1}.

Once **1b** is formed, it interconverts to **1c** and **1d** rapidly because of the negligible barriers connecting them. Therefore, in the calculation of k_6 densities of states of these three isomers were added in the denominator of Eq. (1) [27]. Since **1c** is a chiral molecular ion, its contribution to the state density is doubled. The contributions of other isomers such as **1h**, **1e**, **1i**, and **1j** were negligible. The individual rate-energy dependences thus calculated are shown in Fig. 7. For k_3, the results for the three cases of looseness, A, B, and, C are depicted, which correspond to $\Delta S^{\ddagger}_{1000\,K}$ of 46, 29, and 13 J mol^{-1} K^{-1}, respectively. As shown in the figure, interconversion between **1a** and **1b** is faster than the dissociation of **1a** at low energies. As a consequence, the observed rate constant for the dissociation of **1** would be lower due to the contributions of the states densities of **1b**, **1c**, and **1d**. Including these contributions decreased k_3 and k_4 by a factor of 0.7. It is notable that the contributions of the isomers other than **1a** to the dissociation rates are small, although a total of 12 species can equilibrate with **1a** considering the path degeneracy 3 for reaction 5. This is because the density of states of **1a** is far larger than those of the other isomers at the same energy due to its vibrational modes with relatively low frequencies and the internal rotation of the SiH_3 group.

The rate-energy relation for reaction 3 depends largely on the activation entropy as shown in Fig. 7. From the branching ratio (2.8) of the H_2 and H losses obtained in the MID of **1**, the degree of looseness of the TS for reaction 3 can be chosen. The rate constants corresponding to the present MID are in the range of 10^4–10^6 s^{-1}. As will be described below, reactions 3 and 4 are the main channels in the H and H_2 losses, respectively. Thus, the branching ratio calculated from the corresponding rate-energy curves in the range of (k_3

$+ k_4) = 10^4$–$10^6\ s^{-1}$ should explain the experimental branching ratio. Approximately, TSs for reaction 3 with $\Delta S^{\ddagger}_{1000\,K}$ of 29–46 J mol^{-1} K^{-1} (7.0–11 eu) are acceptable considering the branching ratio. In other words, the reasonable rate-energy curve for reaction 3 lies between the curves k_{3A} and k_{3B} in Fig. 7 (prior to the correction for the 'observed' rate). It seems to be not so meaningful to determine a particular value of the activation entropy because one branching ratio was used here and the critical energies used depend on only theoretical expectations. Because of this uncertainty in the looseness of TS without a saddle point, detailed RRKM analyses were not performed for the direct bond cleavages other than for reaction 3, which in any case are less important. We find that the acceptable TS for the Si–H bond cleavage is somewhat looser than those for typical direct bond cleavages, and we note that McAdoo and co-workers [31–34] have suggested that some C–H or C–Cl bond cleavages occur via a TS tighter than those for typical direct bond cleavages.

The rate constants for the other isomerization and dissociation channels were calculated. Only the results for the respective reactions that can compete most effectively with reactions 6, 4, and 3 will be described. The results calculated at the **1a** energy of 250 kJ mol^{-1} are as follows. The rate constant for the isomerization **1b** → **1h** was 30 times smaller than for **1b** → **1a**. The H_2 loss via **TS1b3a** occurs slower than via **TS1a3a** by 2.5 orders of magnitude. The formation of **2d** by H loss occurs slower than of **2a** by 3.5 orders of magnitude assuming similar looseness for the Si–H cleavages. It is concluded that only reactions 3–6 and interconversion of **1b**, **1c**, and **1d** are important in the primary dissociation of **1**.

To summarize the rate calculations of the primary dissociation of **1**, **1a** can undergo rapid interconversion to **1b**, **1c**, and **1d** at low energies up to about 250 kJ mol^{-1} prior to dissociation. At energies higher than about 450 kJ mol^{-1}, the dissociation mainly occurs without the interconversion. Slightly above the dissociation threshold of **1**, the main dissociation channel is **1a** → **3a** + H_2. As the internal energy increases, the dissociation **1a** → **2a** + H$^{\bullet}$ occurs competitively and dominates over the H_2 loss at high energies.

3.3.2. Secondary dissociation

The secondary dissociation to produce **4** can occur from both **2** and **3** as mentioned above. **2a** produced from **1a** can undergo isomerization prior to further dissociation. (Fig. 5) The individual RRKM rate constants for the following reactions were calculated. (Fig. 8)

$$\mathbf{2a} \rightarrow \mathbf{4} + H_2, \quad k_7 \tag{7}$$

$$\mathbf{2a} \rightarrow \mathbf{2b}, \quad k_8 \tag{8}$$

$$\mathbf{2b} \rightarrow \mathbf{2a}, \quad k_9 \tag{9}$$

$$\mathbf{2b} \rightarrow \mathbf{4} + H_2, \quad k_{10} \tag{10}$$

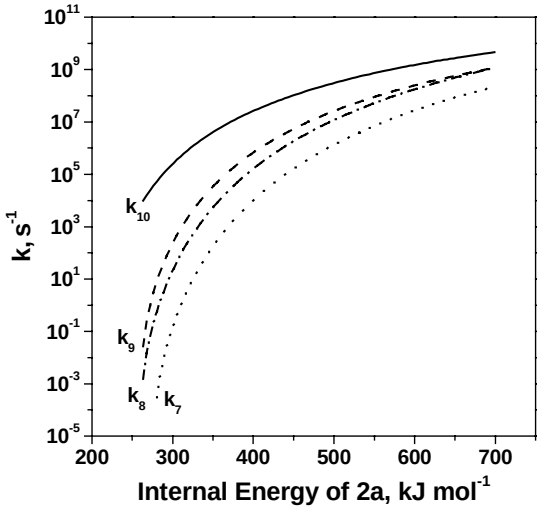

Fig. 8. RRKM rate constants for reactions 7–10 as a function of internal energy of **2a**. k_7–k_{10} denote the rate constants for reactions 7–10, respectively.

The σ values used in the calculations of k_7–k_{10} are 2, 4, 2, and 2, respectively. The contributions from the rapid interconversion of **2b** with the other isomers prior to dissociation or the isomerization to **2a** were included in the calculations. The isomerization **2a** → **2b** occurs far faster than the direct dissociation **2a** → **4** + H_2, and once **2b** is formed it undergoes very fast H_2 loss as shown in Fig. 8. This is a typical double well problem. The solution of coupled differential equations for the production rates for the two dissociation channels can be found elsewhere [27,35]. Only its result will be mentioned here. The overall dissociation rate is approximately determined by the forward isomerization k_8, and almost all of ions **2a** with enough energies dissociate via **2b** and **2c**. The large kinetic energy release (Fig. 2b, $T_{0.5}$ = 0.98 eV) in the MID of **2** by H_2 loss can be understood from the large reverse barrier (92 kJ mol^{-1}) in the step **2a** → **4** + H_2 and the large excess energy ($E - E_0$, about 130 kJ mol^{-1}) expected for the MID from the k_8 curve. The H losses from **2a** and **2b** are energetically less favorable as mentioned in Section 3.2.2, agreeing with the negligible detection of **3** in the MID of **2**.

The analyses described so far lead to the conclusion that **2a** is the only stable isomer among several isomers of **2** that can be formed from the phenylsilane ion. This disagrees with the previous suggestions [6,9] that two different sorts of structural isomer of **2**, 'reactive' and 'unreactive', are formed. As mentioned in Section 3.3.1, in the primary dissociation of **1** the formation of the isomers other than **2a** is energetically far less favorable. Although a stable **2b** ion can be formed from **2a** if the isomerization barrier lies below the barrier (**TS2b4**) for the H_2 loss from **2b**, unlike **TS2a2b** mentioned above, such a pathway could not be found in the present DFT calculation. It is to be noted that the barrier (263 kJ mol^{-1}) obtained for this isomerization, occurring by 1,2 shift of the α-H atom from the silicon to the *ipso*-carbon, is far higher than those for

the isomerizations of **1a** and **3a**, 74 and 106 kJ mol^{-1}, respectively. This higher barrier mainly arises from the particular stability of **2a** enhanced by delocalization of charge over the phenyl ring and the Si atom with participation of the 3p Si orbital orthogonal to the phenyl ring. Accordingly, the energy (279 kJ mol^{-1}) needed for the direct dissociation of **2a** is also larger than those of **1a** and **3a**, 128 and 195 kJ mol^{-1}, respectively. According to IRC calculations, in the course to reach the TSs for the isomerizations from **1a** and **3a** the Si atom is in the plane of the phenyl ring maintaining the C_S symmetry. In the reaction to reach **TS2a2b** from **2a**, however, the C_{2V} symmetry of **2a** is broken by large deformation of the Si–C bond. The Si atom escapes from the phenyl plane asymmetrically to the two *ortho*-carbons. The angle of SiCC and the corresponding dihedral angle of SiCCC of **TS2a2b** are 105.8 and 152.0 degrees, respectively. It is reasonable that a larger energy is needed for such large structural deformation. Maintaining the molecular symmetry as C_S, a structure was optimized for the TS, but it was higher in energy than **TS2a2b** and had two vibrational modes of imaginary frequency. Beauchamp and co-workers [6] reported the yields of the reactive and unreactive isomers of **2** obtained by varying the electron energy used in the EI of phenylsilane. The unreactive isomer is produced dominantly at low energies, from the appearance of **2**, and its relative abundance decreases as increasing energy. Since it was found in the present analysis that **2a** is the predominant isomer formed from the phenylsilane ion, apparently at low energies, the unreactive isomer can be assigned as **2a**. It is hard, however, to assign the reactive one as the other isomers such as **2b**, **2c**, and **2d** because even at higher energies the formation of stable isomers other than **2a** is unfavorable. Therefore, it is proposed that the unreactive and reactive ions would have the identical structure **2a**. It is possible that **2a** at relatively low internal energy, which can be assigned as the unreactive isomer, does not actively undergo reactions with other molecules.

The dissociation of **3a** is rather simple. At moderate energies, **3a** completely equilibrates with **3b** and **3d**. At the energy of the dissociation threshold by H loss from **3a**, the forward and backward isomerization rate constants calculated are 5 $\times$ 10^8 and 7 $\times$ 10^7 s^{-1}, respectively. Since the isomerization barrier lies below the dissociation limit, it is possible to form stable **3b** and **3d** ions that can be assigned as the 'unreactive' isomer of **3** suggested by the ion–molecule experiments [6,9]. The H loss from **3a** is dominant over that from **3b** because the latter is less favorable both energetically and entropically because of a reverse barrier. The lack of Si$^{\bullet+}$ in the MID of **3** indicates that the benzene loss, being energetically similar with the H loss, is entropically less favorable.

3.3.3. Overall reaction mechanism

The production of **4** via **3a** is more favorable than via **2a** since the overall barrier (energy for **1a** $\rightarrow$ **4** + H_2 + H$^{\bullet}$, 288 kJ mol^{-1}) for the former is far lower than that for **1a** $\rightarrow$ **TS2a2b** + H$^{\bullet}$ + H_2 (422 kJ mol^{-1}). Up to internal energy of 422 kJ mol^{-1} or slightly higher this is true because the dissociation via **2a** is not accessible energetically. At higher energies, however, the dissociation via **2a** is more favorable since according to RRKM calculations (Fig. 7) the production of **2a** from **1a** largely dominates over that of **3a**. The contributions of these two channels to the EI mass spectrum of phenylsilane depend on the internal energy distribution of the molecular ion deposited by ionization, which cannot be easily determined. The main pathways for the formation of several isomeric $C_6H_nSi^+$ (n = 5–8) ions determined in the present study are summarized in Fig. 9.

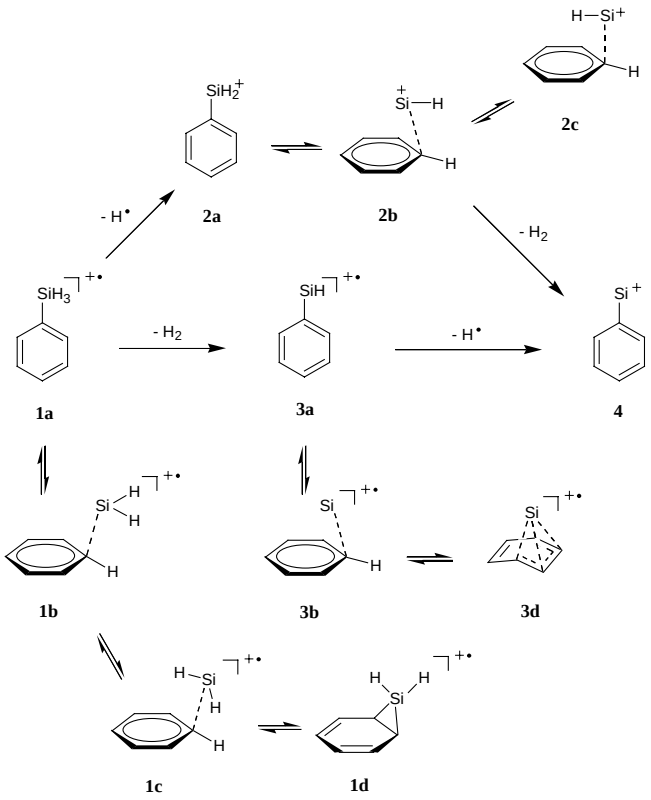

Fig. 9. Main pathways proposed for the formation of several isomers of **1**–**4**.

3.4. Comparison with toluene molecular ion

As is well known, both the benzyl and tropylium ions are produced from the toluene molecular ion by H loss [20]. The present theoretical result predicts that the phenylsilyl ion (**2a**), the silicon analogue of the benzyl ion, is the main product formed by H loss. The difficulty in forming the silacycloheptatrienyl ion (**2d**), the silicon analogue of the tropylium ion, is mainly due to its lower stability as compared to the phenylsilyl ion, while the reverse is true for their carbon analogues [20].

As mentioned above, the $[M-2]^{\bullet+}$ and $[M-3]^+$ ions are hardly formed from the toluene ion unlike the phenylsilane ion. This is mainly due to the difficulty of H_2 elimination from the toluene ion. In the case of the phenylsilane ion, the

endoergicity and critical energy for the 1,1-H_2 elimination are smaller than the energy needed for the H loss. (Fig. 4) By contrast, the endoergicity for 1,1-H_2 elimination from the toluene ion is larger than those for the formation of benzyl and tropylium ions by 35 and 70 kJ mol^{-1}, respectively, according to the UB3LYP/6-311++G(d,p) DFT calculations (J.C. Choe, unpublished results). In addition, attempts to locate the TS for the H_2 elimination failed, implying a very high barrier. A similar difference in 1,1-H_2 elimination was found in a report by comparative EI experiments on CH_4 and SiH_4 by Morrison and Traeger [36]. The appearance energy of $CH_2^{\bullet+}$ was larger than that of CH_3^+ as well as than that of $CH_4^{\bullet+}$, while that of $SiH_2^{\bullet+}$ was the smallest in the products generated by ionization of SiH_4. The difference in behavior for the 1,1-H_2 eliminations is mainly due to the characteristic differences between the two atoms. Silicon is larger in size and its bonding orbitals are more diffuse than carbon. This leads to longer and more easily bent bonds, which can reach a TS for 1,1-H_2 elimination with a smaller energy requirement.

4. Conclusions

From the present MID and theoretical investigations, the overall mechanism for the formation of several isomers of **1**–**4** from the phenylsilane ion has been deduced. It was revealed that **2** and **3** are formed in the primary dissociation of the phenylsilane ion, and both of them can produce **4**. It is expected that at low energies **4** is produced exclusively from **3**, while at high energies its production from **2** is more probable. It was found that **2a** and **3a** were the main product ions in the primary dissociation. It is interesting to note that all of ions **1a**, **2a**, and **3a**, which have the structure of $C_6H_5SiH_x^+$ (x = 3–1), undergo isomerizations easily to ion–molecule complexes $C_6H_6{\cdot}SiH_{x-1}^+$ by 1,2 shift of an α-H atom from the silicon to the *ipso*-carbon. The ion–molecule complexes can form more stable other isomers, return to the original isomers, or undergo dissociation. The various isomers of **2** and **3** cannot be formed by the dissociation of **1** but from **2a** and **3a**, respectively. It is predicted, however, that the isomers formed from **2a** are unstable and dissociate rapidly. According to the present theoretical result, it is hard to form seven- or five-membered rings in ions **1**–**3** from the phenylsilane ion. The present study shows that MID data, which are obtained easily with a conventional tandem mass spectrometer, together with quantum chemical and transition state theoretical calculations, can be used to understand ionic dissociation mechanism, especially when more than one product ions are formed by competitive dissociations.

Acknowledgements

This work was supported by the Korea Research Foundation Grant (KRF-2003-015-C00280). The author thanks Professor Myung Soo Kim of Seoul National University for the use of the mass spectrometer and Hyun Jung Cha and Kyung Mi Choi for assistance in theoretical calculations.

References

[1] H. Schwarz, in: S. Patai, Z. Rappoport (Eds.), The Chemistry of Organic Silicon Compounds, Wiley, Chichester, 1989 (Chapter 7).
[2] J.A. Stone, Mass Spectrom. Rev. 16 (1997) 25.
[3] M.E. Freeburger, B.M. Hughes, G.R. Buell, T.O. Tiernan, L. Spialter, J. Org. Chem. 36 (1971) 933.
[4] F. Bohlmann, C. Köppel, H. Schwarz, Org. Mass Spectrom. 9 (1974) 622.
[5] S. Murthy, Y. Nagano, J.L. Beauchamp, J. Am. Chem. Soc. 114 (1992) 3573.
[6] Y. Nagano, S. Murthy, J.L. Beauchamp, J. Am. Chem. Soc. 115 (1993) 10805.
[7] A. Nicolaides, L. Radom, J. Am. Chem. Soc. 116 (1994) 9769.
[8] A. Nicolaides, L. Radom, J. Am. Chem. Soc. 118 (1996) 10561.
[9] R.L. Jarek, S.K. Shin, J. Am. Chem. Soc. 119 (1997) 6376.
[10] J.C. Choe, Rapid Commun. Mass Spectrom. 17 (2003) 207.
[11] W.N. Allene, F.W. Lampe, J. Am. Chem. Soc. 99 (1977) 2943.
[12] D.K. Bohme, S. Wlodek, H. Wincel, J. Am. Chem. Soc. 113 (1991) 6396.
[13] R. Srinivas, J. Hrušák, D. Sülzle, D.K. Böhme, H. Schwarz, J. Am. Chem. Soc. 14 (1992) 2802.
[14] D. Leblanc, H. Nedev, H.E. Audier, Int. J. Mass Spectrom. 219 (2002) 537.
[15] H.E. Audier, J. Fossey, J.P. Denhez, J.P. Jacquet, P. Mourgues, Int. J. Mass Spectrom. 227 (2003) 381.
[16] R. Srikanth, K. Bhanuprakash, R. Srinivas, C.Y. Wong, J.K. Terlouw, J. Mass Spectrom. 39 (2004) 303.
[17] S. Tajima, D. Watanabe, S. Nakajima, O. Sekiguchi, N.M.M. Nibbering, J. Mass Spectrom. 37 (2002) 299.
[18] S. Calderan, P. Carbone, L. Operti, R. Rabezzana, G.A. Vaglio, J. Mass Spectrom. 37 (2002) 1205.
[19] NIST Chemistry WebBook: NIST Standard Reference Database Number 69, July 2003 Release.
[20] C. Lifshitz, Acc. Chem. Res. 27 (1994) (and references therein).
[21] L. Heydorn, P.C. Burgers, P.J.A. Ruttink, J.K. Terlouw, Int. J. Mass Spectrom. 227 (2003) 453.
[22] R.A. Ochran, P.M. Mayer, Int. J. Mass Spectrom. 227 (2003) 471.
[23] J.C. Choe, Int. J. Mass Spectrom. 235 (2004) 15.
[24] R.G. Cooks, J.H. Beynon, R.M. Caprioli, G.R. Lester, Metastable Ions, Elsevier, Amsterdam, 1973.
[25] M.J. Frisch, G.W. Trucks, H.B. Schlegel, G.E. Scuseria, M.A. Robb, J.R. Cheeseman, V.G. Zakrzewski, J.A. Montgomery Jr., R.E. Stratmann, J.C. Burant, S. Dapprich, J.M. Millam, A.D. Daniels, K.N. Kudin, M.C. Strain, O. Farkas, J. Tomasi, V. Barone, M. Cossi, R. Cammi, B. Mennucci, C. Pomelli, C. Adamo, S. Clifford, J. Ochterski, G.A. Petersson, P.Y. Ayala, Q. Cui, K. Morokuma, N. Rega, P. Salvador, J.J. Dannenberg, D.K. Malick, A.D. Rabuck, K. Raghavachari, J.B. Foresman, J. Cioslowski, J.V. Ortiz, A.G. Baboul, B.B. Stefanov, G. Liu, A. Liashenko, P. Piskorz, I. Komaromi, R. Gomperts, R.L. Martin, D.J. Fox, T. Keith, M.A. Al-Laham, C.Y. Peng, A. Nanayakkara, M. Challacombe, P.M.W. Gill, B. Johnson, W. Chen, M.W. Wong, J.L. Andres, C. Gonzalez, M. Head-Gordon, E.S. Replogle, J.A. Pople, Gaussian 98 (Revision A.11.3), Gaussian Inc., Pittsburgh, PA, 2002.
[26] A.P. Scott, L. Radom, J. Phys. Chem. 100 (1996) 16502.
[27] T. Baer, W.L. Hase, Unimolecular Reaction Dynamics: Theory and Experiments, Oxford, New York, 1996.
[28] F.W. McLafferty, F. Tureček, Interpretation of Mass Spectra, Fourth ed., University Science Books, Mill Valley, 1993.
[29] G. Portalone, A. Ramondo, A. Domenicano, I. Hargittai, J. Organomet. Chem. 560 (1998) 183.

[30] C. Lifshitz, Adv. Mass Spectrom. 11 (1989) 713.
[31] D.J. McAdoo, S. Olivella, A. Sole, J. Phys. Chem. A 102 (1998) 10798.
[32] L.L. Griffin, J.C. Traeger, C.E. Hudson, D.J. McAdoo, Int. J. Mass Spectrom. 217 (2002) 23.
[33] C.E. Hudson, D.J. McAdoo, L.L. Griffin, J.C. Traeger, J. Am. Soc. Mass Spectrom. 14 (2003) 136.
[34] C.E. Hudson, J.C. Traeger, L.L. Griffin, D.J. McAdoo, J. Phys. Chem. A 107 (2003) 512.
[35] J.J. Butler, M.L. Fraser-Monteiro, L. Fraser-Monteiro, T. Baer, J.R. Hass, J. Phys. Chem. 86 (1982) 747.
[36] J.D. Morrison, J.C. Traeger, Int. J. Mass Spectrom. Ion Phys. 11 (1973) 289.